

Dynamic nuclear polarization of ^{13}C in aqueous solutions under ambient conditions

Mark D. Lingwood, Songi Han*

Department of Chemistry and Biochemistry, University of California, Santa Barbara, CA 93106, United States

ARTICLE INFO

Article history:

Received 2 December 2008

Revised 1 August 2009

Available online 6 September 2009

Keyword:

Dynamic nuclear polarization, DNP

Hyperpolarization

Overhauser effect

Three-spin effect

^{13}C

ABSTRACT

The direct enhancement of the ^{13}C NMR signal of small molecules in solution through Overhauser-mediated dynamic nuclear polarization (DNP) has the potential to enable studies of systems where enhanced signal is needed but the current dissolution DNP approach is not suitable, for instance if the sample does not tolerate a freeze-thaw process or if continuous flow or rapid re-polarization of the molecules is desired. We present systematic studies of the ^{13}C DNP enhancement of ^{13}C -labeled small molecules in aqueous solution under ambient conditions, where we observe both dipolar and scalar-mediated enhancement. We show the role of the three-spin effects from enhanced protons on ^{13}C DNP through DNP experiments with and without broadband ^1H decoupling and by comparing DNP results with H_2O and D_2O . We conclude that the efficiency of ^{13}C Overhauser DNP in small molecules strongly depends on the distance of closest approach between the electron and ^{13}C nucleus, the presence of a scalar contribution to the coupling factor, and the magnitude of the three-spin effect due to adjacent polarized protons. The enhancement appears to depend less on the translational dynamics of the ^{13}C -labeled small molecules and radicals.

© 2009 Elsevier Inc. All rights reserved.

1. Introduction

Nuclear magnetic resonance (NMR) of ^{13}C is vitally important as a spectroscopic tool for biological systems because of its non-invasive nature and wide range of available information. However, ^{13}C magnetic resonance suffers from an inherent lack of sensitivity due to its low gyromagnetic ratio and natural abundance. This has led researchers to seek methods of highly enhancing the NMR signal of target nuclei. An increasingly popular approach is the amplification of NMR signal through dynamic nuclear polarization (DNP), which combines the principles of NMR and electron spin resonance (ESR). In DNP, the orders-of-magnitude higher polarization of an unpaired electron is transferred to nearby nuclei, resulting in potentially large NMR signal enhancements. In addition to obtaining enhanced NMR signal, DNP can also help simplify the often complex ^{13}C NMR spectra of biological systems, by only enhancing the NMR signals of the ^{13}C sites in close contact with the electron spins.

The initial application of DNP on ^{13}C was the study of collision dynamics in solutions of organic solvents with a small amount of stable radical species [1,2]. Magic angle spinning-DNP (MAS-DNP) experiments on solid samples were presented originally for the purpose of investigating coal [3], then later at higher fields for studying biological samples in frozen solutions [4,5]. Since most biological processes occur in solution, there has been interest in solution-state ^{13}C DNP, initially demonstrated by flowing the sam-

ple from a low polarizing field to a higher NMR detection field [6], and more recently performed by polarizing in the solid state for an extended period of time at 1.2 K, then rapidly dissolving the hyperpolarized sample and delivering it to the system of interest [7]. The latter methodology, known as dissolution DNP, is particularly notable for the extremely high, three to four orders-of-magnitude signal gain. This large signal enhancement has opened up new applications for NMR and magnetic resonance imaging (MRI), because a ^{13}C -containing molecule can be hyperpolarized and easily observed, allowing for fast acquisition of solution spectra or the *in-vitro* or *in-vivo* spectroscopy and imaging of metabolic processes [8,9].

While dissolution DNP has the advantage of providing very large signal, the disadvantage lies in the freeze-thaw sample polarization process and lifetime of the enhanced signal. The samples are polarized at 1.2 K for a few hours, then rapidly dissolved and removed from the polarizing magnet [7]. From that point, the polarization is significant only for approximately four times the length of the longitudinal relaxation time (T_1) of the substance, which is typically between 20 and 60 s when quaternary or carbonyl carbons are used [8,9]. Even when employing multiple smaller and variable angle pulses, the hyperpolarized signal is rapidly consumed, limiting the total observation time for the polarized molecule. Also, many samples including biological systems and volatile molecules do not tolerate the process of freezing and rapid thawing, and thus are not suited for dissolution DNP.

In this paper, we discuss the DNP of dissolved ^{13}C -labeled small molecules, carried out entirely under ambient conditions. While

* Corresponding author. Fax: +1 805 893 4120.

E-mail address: songi@chem.ucsb.edu (S. Han).

polarizing via the Overhauser effect at room temperature provides smaller signal enhancements than dissolution DNP, nuclear polarizations can still be generated that are 2–10 times higher than the thermal polarization in the highest current commercially available magnetic field (21 T). There are numerous situations where modest enhancement still enables new scientific insight into samples that cannot be hyperpolarized otherwise. The time for maximum polarization buildup is five times the T_1 in the liquid state in the presence of radical, where the T_1 is usually less than 10 s, as opposed to hours at 1.2 K. Thus for a system where spectroscopy is performed in the presence of radicals, DNP-enhanced scans can be repeated at a rate of $5 \times T_1$. If the polarized molecule is to be transferred to an external sample for spectroscopy or imaging, the hyperpolarized signal at room temperature is still subject to rapid decay due to the limited polarization lifetime and use of pulses. However, since the polarization process can be repeated much faster than dissolution DNP, multiple and continuous polarizations and transfers can be performed with ~ 1 min repetition rates. This can be advantageous for the study of processes that last longer than $5 \times T_1$, but are shorter than the time it takes to polarize samples at 1.2 K; many enzymatic reactions and metabolic processes fall into this category, especially the observation of chemotherapy or drug effects. The radical can also be attached to a solid support and subsequently filtered from the liquid sample, providing polarized samples with zero residual radical concentration [10]. Hyperpolarized water prepared in this manner and transferred to a system of interest was recently shown to have MRI signal distinct from bulk water in the system [11]; this procedure could be effective for ^{13}C MRI as well. In addition, since the DNP process is carried out entirely at room temperature, the direct polarization of complex biological systems that are unable to withstand cooling to 1.2 K can be performed. The equipment can also be made portable [12], employing either a small permanent magnet or the fringe field of an NMR or MRI magnet at the facility where the experiment is to be performed.

To our knowledge, ^{13}C DNP at room temperature via the Overhauser effect has not been reported for molecules dissolved in water. Here we present a systematic study of the DNP mechanism of different molecules at 0.35 T, discuss the effects of polarization transfer from nearby protons (the three-spin effect), and describe the effect of the solvent and varying proton exchange rates on the NMR signal enhancement of ^{13}C .

2. Theory

Dynamic nuclear polarization can occur through four different mechanisms: the Overhauser effect [1,2], which is the only appreciable effect for liquids, the solid effect [3], which has limited experimental use, and the cross effect/thermal mixing [3,4], which is the predominant effect for contemporary solid-state and dissolution DNP. In this report we focus on DNP in aqueous systems at 0.35 T, so we present only a summary of the Overhauser effect as it relates to the systems of interest.

The Overhauser effect is typically described with the four-level energy diagram shown in Fig. 1. Saturation of the electron transition p can lead to non-equilibrium nuclear polarization through the cross-relaxation mechanisms w_0 or w_2 . If $w_0 > w_2$, the electrons and nuclei undergo scalar coupling, which requires an overlap of the electron and nuclear wavefunctions. For ^{13}C , scalar coupling is more frequently observed in molecules which also contain a halogen atom, or at high fields [13–16]. Scalar coupling is characterized by a non-equilibrium nuclear polarization that gives an enhanced NMR signal with the same sign as the equilibrium, thermally polarized signal (positive enhancement). If the two spins undergo dipolar coupling, $w_2 > w_0$, and DNP-enhanced signal with the

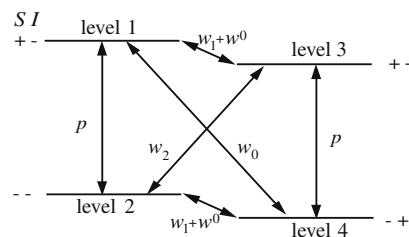


Fig. 1. The four-level energy diagram describing a system of two interacting spins, in this case an electron (S) and a nucleus (I). The intrinsic electron and nuclear relaxation is given respectively by p and w_0 , whereas the dipolar and/or scalar interactions are represented by w_0 , w_1 , and w_2 .

opposite sign of the equilibrium signal is obtained (negative enhancement). Dipolar coupling dominates the DNP for hydrogen nuclei and is quite common for ^{13}C at lower fields. Relaxation can occur through both the w_0 or w_2 transitions at the same time, giving rise to a mixed scalar and dipolar interaction. Dipolar coupling between ^1H and ^{13}C through this same mechanism forms the basis of the nuclear Overhauser effect (NOE), a commonly used method in NMR spectroscopy [17].

The observed NMR signal enhancement, E , is defined as the ratio of the enhanced signal to the equilibrium signal $\langle I_0 \rangle$, and

$$E = \frac{\langle I_z \rangle}{\langle I_0 \rangle} = 1 + \rho f s \frac{\gamma_S}{\gamma_I} \quad (1)$$

where ρ is the coupling factor, f is the leakage factor, and γ_S and γ_I are the gyromagnetic ratios of the electron and nucleus, respectively. The coupling factor, ρ , gives the coupling between the electron and nucleus, can range from -1 (pure scalar coupling) to 0.5 (pure dipolar coupling), and has a strong field dependence [1]. Please note that our definition of ρ is identical to that of ξ in [1], and our usage of ρ is not consistent with how ρ is usually defined when discussing NOE [17]. The coupling factor strongly depends on the translational correlation time, τ_t , between the radical and nucleus of interest. The coupling factor decreases with increasing correlation times [1,18], and previous reports have shown that the dipolar interaction for water [19] and small organic molecules [16] with organic radicals is modulated mainly by translational motion, which leads us to discuss our results in terms of translational instead of rotational correlation. The translational correlation time is a function of the distance of closest approach, d , between the nucleus and radical and their respective diffusion coefficients, D_1 and D_S [1]:

$$\tau_t = \frac{d^2}{D_1 + D_S} \quad (2)$$

The leakage factor, f , relates to the electron's ability to relax the proton, and is given by

$$f = 1 - \frac{T_1}{T_{10}} \quad (3)$$

where T_1 is the longitudinal relaxation time of the system, and T_{10} is the longitudinal relaxation time of the system in the absence of radicals. A leakage factor of 1 implies that all the relaxation of the nucleus is caused by the electron, whereas a leakage factor of 0 occurs when all relaxation of the nucleus is through other sources. The saturation factor in Eq. [1], s , is the degree of saturation of the electron spins, and can vary from 0 to 1, depending on the saturation power applied, the radical used, and nitrogen relaxation rates (for nitroxide radicals) [20]. The saturation factor also strongly depends on the concentration of the radicals because of Heisenberg spin exchange, which broadens the ESR lines and mixes the hyperfine states [21]. At high concentrations of nitroxide radicals

(~20 mM), the maximum value of the saturation factor (s_{\max}) can approach 1 due to Heisenberg exchange. Since s heavily depends on applied microwave power, the observed enhancement can be plotted against applied microwave power and extrapolated to infinite power ($s \rightarrow s_{\max}$); this number is referred to as the maximum enhancement (E_{\max}) [20]

$$E_{\max} = 1 + \rho f s_{\max} \frac{\gamma_s}{\gamma_1} \quad (4)$$

Eq. [1] holds for both NOE and DNP, but is usually rewritten to describe DNP by factoring out the negative gyromagnetic ratio of the electron:

$$E = 1 - \rho f s \frac{|\gamma_s|}{\gamma_1} \quad (5)$$

The ^{13}C DNP described so far arises from direct radical–carbon coupling. However, in most molecules of interest, there are bound or otherwise nearby protons, which themselves experience dipolar enhancement through the Overhauser effect with the radicals, according to Eq. [1]. The NOE between these hyperpolarized protons and carbon can then provide positive enhancement to the carbon through Eq. [1], owing to the positive gyromagnetic ratios of both hydrogen and carbon. In such a ^{13}C , ^1H and radical three-spin system, Eqs. [1] and [5] are no longer valid [1,22,23]. Instead, the equation for DNP in a three-spin system becomes [24]

$$E_2 = 1 + \rho_2^s f_2^s s \frac{\gamma_s}{\gamma_1} + \rho_2^1 f_2^1 \frac{\gamma_1}{\gamma_2} (1 - E_1) \quad (6)$$

where the detected species (carbon) is spin 2 and third species (hydrogen) is spin 1. The second term in the equation is the direct DNP term, as expressed in Eq. [1], with ρ_2^s indicating the coupling factor of spin 2 due to its interaction with the electron spin S . The third term in the equation, the three-spin term, gives enhancement of carbon due to the NOE from a hyperpolarized proton, and includes the NOE interaction and E_1 , which is the DNP enhancement of the proton as given by Eq. [1]. Thus, a simplified version of Eq. [6] would be $E_2 = 1 + \text{DNP term} + \text{three-spin term}$. The DNP term is negative for dipolar coupling and positive for scalar coupling, due to the sign of the coupling factor and the negative γ_s . The three-spin term is always positive, since the interactions between the proton and the carbon and those between the proton and the radical are almost always dipolar, which causes E_1 to be negative and ρ_2^1 to be positive. Thus, the second and third terms offset each other if dipolar relaxation dominates the interaction between the radical and carbon nucleus. The DNP term and three-spin terms add together if scalar relaxation is dominant. The contribution from the three-spin effect will decrease at higher radical concentrations, where the NOE becomes much less effective due to leakage of the carbon relaxation to the radical (f_2^1 goes to zero) [6]. Importantly, the three-spin term of Eq. [6] will become negligible if the protons are fully saturated along with the electrons in a triple resonance experiment, where $E_1 = 0$. The amplitude and sign of the observed signal under double and triple resonant conditions depends on the type of enhancement between the radical and carbon nuclei and the magnitudes of the terms in Eq. [6]. Three cases are possible, and they are listed below and schematically depicted in Fig. 2.

- (a) If dipolar enhancement dominates, and the direct interaction (the DNP term) is larger than the interaction through the proton (the three-spin term), the enhanced signal is inverted with respect to the equilibrium signal when only the electrons are saturated (double resonant). The addition of proton saturation to a DNP experiment, which effectively removes the three-spin term, will increase the overall NMR signal enhancement (Fig 2a).

Expected Signal Upon Saturation of Electrons and Protons:










	Thermal Polarization	Electron Saturation	Electron and Proton Sat.
a) Dipolar coupling, DNP term dominates			
b) Dipolar coupling, three-spin term dominates			
c) Scalar coupling, both cases			

Fig. 2. A schematic to show the signs and magnitudes of the observed NMR signal without DNP enhancement (thermal polarization) with DNP enhancement (electron saturation) and with DNP enhancement and complete proton saturation (electron and proton saturation).

- (b) If dipolar enhancement dominates the DNP term, but the three-spin term dominates Eq. [6], the enhanced NMR signal will have the same sign as the equilibrium signal, even though all the interactions are mainly dipolar. Complete saturation of the protons will give a decreased and inverted NMR signal (Fig. 2b).
- (c) If scalar enhancement dominates the DNP term, the enhanced and equilibrium NMR signal will have the same sign. Saturation of the protons will decrease the signal, regardless of whether the DNP term or three-spin term is larger (Fig. 2c).

It is likely that the carbon nucleus experiences a mixture of dipolar and scalar enhancement from the radical. However, it is difficult to experimentally distinguish the difference between a lower coupling factor due to the effects of mixed dipolar and scalar enhancement versus a lower coupling factor caused by increased correlation times of the ^{13}C species with respect to the radical. Therefore we are only able to determine which type of enhancement dominates the DNP term, and not the extent of mixed relaxation mechanisms.

3. Results and discussion

All DNP, T_1 and diffusion experiments were carried out at 0.35 T, where the electron spin resonance frequency is 9.8 GHz and the ^{13}C NMR frequency is 3.74 MHz.

3.1. Enhancement of ^{13}C in different molecules

The molecule that gave the greatest ^{13}C NMR signal enhancement was urea. The ^{13}C spectra of 5 M ^{13}C -labeled urea, 5 M *N,N*-dimethylformamide (DMF, carbonyl ^{13}C) and 1 M sodium pyruvate, each dissolved in water along with 20 mM of the free radical 4-amino-2,2,6,6-tetramethyl-1-piperidinyloxy (4-amino-TEMPO), are presented in Fig. 3 with and without DNP. The observed urea enhancement (E of Eq. [1]) was -265 fold, with an estimated maximum enhancement (E_{\max} at extrapolated maximum power from Eq. [4]) of -455 . The sign of the enhancement shows that urea undergoes dipolar enhancement. DMF gave $+60$ fold enhancement, and the sign of enhancement and decoupling experiments below show that DMF experiences scalar enhancement. Sodium pyruvate showed -160 fold dipolar enhancement.

The urea maximum enhancement of -455 (corresponding to $\rho = 0.19$ assuming $s_{\max} = 1$) is lower than the maximum possible DNP enhancement for ^{13}C from Eq. [1], which is -1300 in the extreme narrowing dipolar limit (where $\rho = 0.5$). This is due to the correlation times of these molecules being slower than the inverse

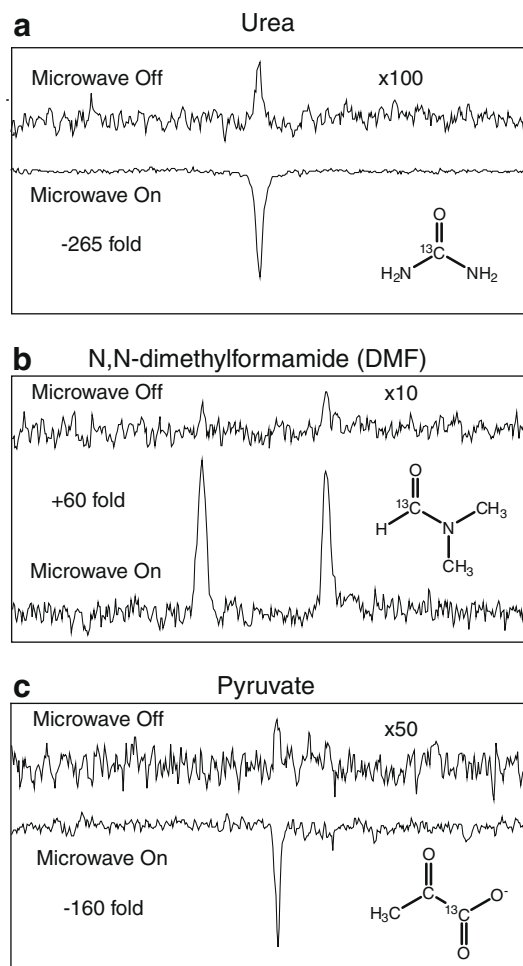


Fig. 3. The enhanced and equilibrium NMR signals are shown for aqueous solutions of urea (a), DMF (b), and sodium pyruvate (c). The unenhanced spectrum is enlarged by a different factor depending on the amount of observed enhancement. The unenhanced (microwave off) and enhanced spectra are the average of 3200 and 8 scans for urea, 6400 and 16 scans for DMF and 18,000 and 64 scans for pyruvate.

of the electron spin Larmor frequency of 9.8 GHz at the magnetic field of 0.35 T (~ 100 ps). Therefore, Overhauser DNP enhancement decreases with increasing fields [1]. As a reference, the coupling factor for water at 0.35 T has been reported to be 0.22 [25]. Since urea has slower dynamics than water, a somewhat lower coupling factor is expected.

Due to the long experimental times required to measure thermally polarized (equilibrium state) signals, it was not feasible to measure the actual or maximum enhancements for every sample. This is due to homebuilt NMR electronics, and the fact that optimal microwave penetration to the sample in an aqueous DNP experiment is obtained for very small sample volumes (4 μL). Instead, urea was chosen as a reference standard, and the value of the other observed enhancements were referenced to a sample of urea. Because of this, the following numbers are expressed as percentages relative to the measured urea signal, and the sign of the enhanced signal relative to its equilibrium signal is specified by the sign of the percentage (Table 1). All samples were dissolved in water at 5 M concentrations, except for sodium pyruvate, which is only soluble to 1 M in water (the numbers reported are relative to 1 M urea).

As seen in Table 1, the urea carbon gave the best signal enhancement, followed by the carbonyl carbon of acetone. The labeled carbonyl carbon in pyruvate gave moderate enhancement, followed by methanol, DMF, and acetone's methyl carbon. All

Table 1

DNP enhancements of different molecules dissolved in water with 20 mM 4-amino-TEMPO, expressed as a percentage relative to the observed enhancement of urea. The percentage change of the signal upon broadband ^1H decoupling is listed, and the product of the middle two columns gives the relative enhancement in the absence of three-spin effects (direct DNP).

Molecule	Relative enhancement (%)	Decoupling, % change (%)	Relative enhancement, direct DNP (%)
Urea	-100	102	-102
Acetone C=O	-80	109	-87
Acetone CH_3	-18	121	-22
Pyruvate	-55	98	-54
Methanol	-27	119	-32
DMF	25	56	14

enhancements were negative, and thus dominated by dipolar interactions, except for DMF, which gave positive scalar enhancement. The sign of the enhancement was determined by either direct measurement of the unenhanced signal or an analysis of the decoupling results. Uniformly ^{13}C -labeled glucose was also tested, but DNP-enhanced signal was barely visible after 512 scans (urea was clearly visible in a single scan). This low enhancement can be attributed to an unfortunate combination of two factors: a low leakage factor for ^{13}C nuclear spins even with high (20 mM) concentrations of radical ($f = 0.25\text{--}0.3$) and the expected presence of a detrimental three-spin effect through the many bound and highly polarized protons; this causes the NOE and DNP terms to be of equal magnitude and offset each other. The error in all measurements is estimated to be 15%, which is sufficient to make qualitative comparisons.

The coupling factor between the radical and ^{13}C , ρ or ρ_2^S , is the physically meaningful parameter that describes the different systems, but due to experimental limitations we are only able to measure changes in E , which gives a sum of the DNP and three-spin terms. We discuss the DNP and three-spin terms separately below and in the next section.

In order to look at the DNP term, we first need to remove the three-spin term. This is accomplished with broadband ^1H decoupling. The change of the signal upon decoupling was measured for each system, and is presented in Table 1 as a percentage change of the integral of the DNP-enhanced signal after the addition of ^1H decoupling. An increase in signal upon decoupling gives a percentage larger than 100. The relative enhancement was multiplied by the change in signal upon decoupling and listed in the rightmost column, which gives the comparison of the DNP term for the different systems.

The DNP term contains the radical – ^{13}C coupling factor as a product with the saturation and leakage factors. To relate the DNP component of E to changes in the coupling factor, we first assume the saturation factor, s , to be the same for all measurements. The same microwave power was used for all measurements, and care was taken to use the same amount of samples and place them in the same position inside the microwave cavity. Thus, we assume that the same amount of microwave power reaches the samples for each experiment, but this alone does not imply that the saturation factor is equal for all samples. We also can assume that $s_{\text{max}} \approx 1$ for all systems. This is because, for nitroxide radicals at high concentrations, Heisenberg spin exchange effectively mixes the hyperfine states allowing the maximum possible saturation factor, s_{max} , to approach 1 [20,21]. To decide at which radical concentration $s_{\text{max}} \approx 1$ for all systems, the Heisenberg spin exchange rate was experimentally determined for the most viscous system, 5 M DMF, to be $1.96 \times 10^6 \text{ mM}^{-1} \text{ s}^{-1}$ by measuring the ESR linewidth vs. concentration [26]. The spin exchange rate was then used to calculate s_{max} at a given concentration [20]; concentrations of 20 mM were chosen for all measurements because it was the

Table 2

The second column gives the DNP enhancement values from Table 1. The ESR linewidths are listed for reference, and T_1 and T_{10} are the longitudinal relaxation times of the system with and without radical, respectively. The leakage factor and corrected relative enhancement are explained in the text. The far right column directly relates to changes in the coupling factor between systems.

Molecule	Relative enhancement, direct DNP (%)	ESR Linewidth (G)	T_1	T_{10}	Leakage (f)	Relative Enhancement, f corrected (%)
Urea	-102	2.27	3.40	35	0.90	-102
Acetone C=O	-87	2.63	3.36	23.7	0.86	-91
Acetone CH ₃	-22	2.63	2.42	16.5	0.85	-23
Pyruvate	-54	2.21	2.69	36.2	0.93	-52
Methanol	-32	2.41	2.7	12.4	0.78	-37
DMF	14	2.21	1.70	6.92	0.75	17

lowest radical concentration where s_{\max} was sufficiently close to 1 ($s_{\max} = 0.95$). Solutions of lower viscosity will have s_{\max} even closer to 1 [20,21], allowing us to assume that applying the same microwave power results in the same saturation factor. This is a fair approximation, but does not account for the slightly increased saturation factor from a narrower ESR line. For this reason, ESR linewidths are also reported in Table 2. It can be seen that this is a small contribution, as changes in enhancement do not directly follow changes in linewidth. While s_{\max} is close to 1, the actual saturation parameter s is limited by the amount of microwave power we can use without sample heating. We estimate that our actual saturation $s \approx 0.6$, based on a comparison of the urea enhancement and E_{\max} values. In addition, we can easily measure the leakage factor, f , and we correct the observed enhancement for differences between the leakage factors by applying a correction factor to each measurement: $E_{\text{corrected}} = E_{\text{observed}} \times (f_{\text{urea}}/f_{\text{sample}})$. This is shown in the far right column of Table 2, where the percentages directly relate to changes in the coupling factor between the radical and the carbon nuclei.

3.2. The three-spin effect

The addition of broadband proton saturation to the experiments above can help to describe the influence of the three-spin term in Eq. [6], in addition to providing an increase in NMR signal in some cases. Decoupling DNP experiments were performed on urea and DMF as a function of the radical concentration. The results are shown in Fig. 4, where the results are reported as a percentage between the integral of the enhanced signal with ¹H decoupling applied and the enhanced signal integral without decoupling. An increase in signal upon decoupling gives a percentage greater than 100, a decrease in signal when decoupling is added gives a percentage less than 100. Note that in this presentation of Fig. 4, the percentage only reflects the appearance of the signal before and after decoupling, where the signal before decoupling is given the value of +100% for both urea and DMF, even though urea displays nega-

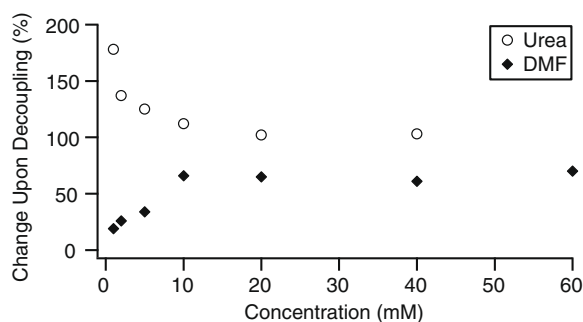


Fig. 4. Ratio of the enhanced NMR signal with broadband ¹H decoupling to the enhanced signal without decoupling, as a function of 4-amino-TEMPO concentration. The open circles represent urea, and the filled diamonds represent DMF.

Table 3

Ratio of enhanced NMR signal with broadband ¹H decoupling to the enhanced signal without decoupling for solutions with a 2 mM concentration of 4-amino-TEMPO. The negative sign of the acetone methyl carbon indicates that the signal changed sign with decoupling. The sign of each signal with respect to thermal equilibrium is not specified.

Molecule	2 mM decoupling (%)
Urea	131
Acetone C=O	101
Acetone CH ₃	-128
Pyruvate	158
Methanol	232
DMF	26

tive enhancement and DMF shows positive enhancement of a lower magnitude.

As seen in Fig. 4, urea gave larger enhancement upon decoupling at low concentrations of radical. This further shows that the DNP term in Eq. [6] is the dominant term for urea, and that if low concentrations of radical are used, decoupling can be applied to enhance signal. At high concentrations of radical, the three-spin effect is no longer effective due to the radical's disruption of the NOE. Fig. 4 also shows that the signal for DMF became smaller with the addition of proton decoupling at all radical concentrations. Since proton decoupling at high radical concentrations still altered the signal, the proton-carbon NOE is appreciable for DMF even at high radical concentrations. The observation that the sign of the DNP signal did not change upon efficient proton decoupling at any radical concentration indicates that the radical-carbon interactions are scalar in nature (the DNP term is positive).

The effect of proton decoupling was tested for all molecules co-dissolved with 20 mM (Table 1) and 2 mM (Table 3) concentrations of 4-amino-TEMPO in order to examine the magnitude of the three-spin effect. The decoupling percentage is reported as negative if the signal inverts upon decoupling. Table 3 shows that at 2 mM radical concentrations, the DNP term dominates for urea, the acetone carbonyl carbon, pyruvate and methanol, whereas the three-spin term dominates for the methyl carbons of acetone. DMF undergoes scalar enhancement, and since the signal decreased by more than 50% upon proton decoupling, the three-spin term is larger than the DNP term at 2 mM radical concentrations.

3.3. Solvent effects and chemical exchange

Next we would like to discuss the effects of intermolecular NOE from solvent molecules, distinct from the NOE effects through bound protons. We chose urea and DMF for this analysis, because the amide protons on urea undergo chemical exchange with the solvent while the protons on DMF do not.

To consider urea, we first investigate the effect of the amide proton exchange rate on DNP and determine whether the large enhancement of urea is due chemical exchange. The rate of exchange varies with pH, and is the smallest at pH 7 (the inverse

Table 4

The DNP enhancement of urea solutions at pH 4 and 10, referenced to a pH 7 solution. The relative enhancement was corrected for differences in the leakage factors.

pH	2 mM relative enhancement (%)	20 mM relative enhancement (%)
4.0	102	94
7.0	100	100
10.0	97	98

lifetime of a proton on urea is about 1 s^{-1} at pH 7) and increases at pH 4 as well as pH 10 (1380 s^{-1} and 250 s^{-1} , respectively) [27]. The DNP-enhanced signal of 5 M urea solutions at pH 4 and 10 was compared to the enhancement at pH 7. Both 2 mM and 20 mM concentrations of 4-amino-TEMPO were used, so that situations with and without a large three-spin effect can be compared. The results are shown in Table 4. There is no observed change within the experimental error, showing that the exchange rate does not play a role in the magnitude of DNP enhancements. This is likely due to the fact that the lifetime of the amide proton on urea, which is at most 1 s at pH 7, is shorter than the time required to affect the polarization of the ^{13}C nucleus that reaches full polarization after five times the ^{13}C T_1 , thus on the order of tens of seconds and longer. It would be plausible that the amide protons have a much smaller NOE to the carbonyl carbon than the water protons, so that the influence of the three-spin effect from amide protons would be minimal even if the proton residence time is long.

To describe the influence of the intermolecular three-spin effect due to solvent protons, the DNP enhancement of 5 M urea and 5 M DMF were compared in water and D_2O . Based on Eq. [6], there should be a three-spin effect from the water protons to the carbon that is not present when the molecules are dissolved in D_2O . This difference would be pronounced at low radical concentrations and minimal at radical higher concentrations, because f_2^j in Eq. [6] decreases as concentration is increased. The comparison between solvents is shown in Fig. 5, where the signal in D_2O , corrected for leakage factor differences, was divided by the signal in H_2O , then multiplied by 100% for presentation as a percentage. Again, the percentage does not specify the sign of the unenhanced signal, so both urea and DMF have a positive percentage. For urea, there was greater DNP enhancement when dissolved in D_2O than H_2O , but only at low radical concentrations, because a disadvantageous three-spin effect was removed. Note that deuterated urea was not used, so the protons originally on the solid urea exchange with the deuterons in solution to provide a non-negligible concentration of HDO and H_2O . It is expected that the enhancement in D_2O would be even greater if deuterated urea is used. The effect of proton decoupling versus $\text{D}_2\text{O}/\text{H}_2\text{O}$ exchange on the DNP enhancement of urea is comparable, because the NOE effects of the solvent versus bound protons cannot be differentiated for fast

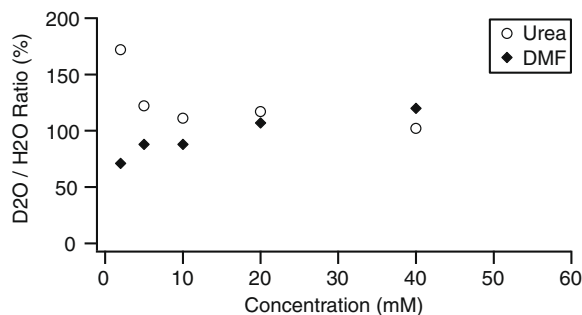


Fig. 5. Ratio of the enhanced NMR signal of molecules dissolved in D_2O to that of molecules dissolved in H_2O , as a function of 4-amino-TEMPO concentration. The open circles represent urea, and the filled diamonds represent DMF.

Table 5

Diffusion coefficients of the solute, D_i , and the radical, D_s , compared to the relative enhancement corrected for proton decoupling and leakage factor differences. All samples are 5 M aqueous solutions with 20 mM of 4-amino-TEMPO radical.

Molecule	D_i ($10^{-9} \text{ m}^2/\text{s}$)	D_s ($10^{-9} \text{ m}^2/\text{s}$)	$D_i + D_s$ ($10^{-9} \text{ m}^2/\text{s}$)	Relative enhancement (%)
Urea	1.07	0.32	1.39	-102
Acetone C=O	1.10	0.27	1.37	-91
Acetone CH_3	1.10	0.27	1.37	-23
Methanol	1.36	0.26	1.62	-37
DMF	0.68	0.18	0.86	17

exchanging protons. There effect of $\text{D}_2\text{O}/\text{H}_2\text{O}$ exchange on the DNP enhancement of DMF was clearly visible, but smaller compared to the effect of proton decoupling. This result shows that there a substantial amount of three-spin effect from the proton bound to the carbon that does not undergo chemical exchange with the solvent. However, we also determined that the solvent protons have non-negligible intermolecular NOE effects on the ^{13}C DNP of DMF.

3.4. Contributions to the coupling factor

Finally we discuss the contributions to the radical- ^{13}C coupling factor for the different molecules studied. As discussed in Section 3.1, the percentages presented in the rightmost column of Table 2 directly give the differences between the coupling factors. Two causes could be responsible for the variance in coupling factors, either different correlation times or a different mixture of scalar and dipolar enhancement for each molecule. The experimental separation of these contributions is difficult, but we can discuss individual factors affecting the correlation times.

In order to consider the relative importance of the components of the correlation time, we assume that the dipolar enhancement is mainly modulated by translational motions [16]. The coupling factor decreases as the translational correlation time increases, and τ_c is related to the distance of closest approach and the diffusion coefficients of the ^{13}C containing molecule and the radical as shown in Eq. [2]. To separate these components, we compare the sum of the translational diffusion coefficients of the nucleus, D_i , and the radical, D_s , to the observed DNP enhancement in Table 5. The diffusion coefficients for 5 M solutions of acetone, DMF and methanol were measured by the standard pulsed field gradient spin echo (PGSE) method, and the diffusion coefficients of urea and the 4-amino-TEMPO radical were calculated from literature values through a procedure which is discussed in the experimental section. According to Eq. [2], a larger diffusion coefficient gives a smaller correlation time, which results in an increased coupling factor. The easiest comparison is between urea and acetone, because they have a nearly equal sum of diffusion coefficients. The carbonyl carbons of urea and acetone have nearly equal DNP enhancements, which makes sense given their very similar molecular structure. However, urea and the methyl carbons of acetone have very different enhancement even with the removal of the three-spin effects, suggesting that the change in correlation time and enhancement is not determined by diffusion but instead driven by molecular structure, and thus the distance of closest approach between the radical and nucleus. This idea is supported by the diffusion values of the other systems presented in Table 5, especially methanol, which has a higher diffusion coefficient but lower enhancement. The methyl carbon of acetone and methanol would likely have a larger distance of closest approach due to the hindrance of the bound protons, which would increase the translational correlation time and decrease enhancement. It is unclear if the enhancement of DMF can be interpreted with translational diffusion coefficients, since scalar enhancement requires the overlap of the electron and nucle-

ar wavefunctions, and thus closer molecular contact for a longer period of time than dipolar enhancement. Thus, DMF may form complexes with the radical that are long-lived compared to the translational correlation times, which could be governed by rotational correlation times [1]. Regardless, our finding that the distance of closest approach seems to play a large role in determining the translational correlation time, and thus enhancement, is a generally useful insight relevant for DNP via other mechanisms, such as the thermal mixing effect commonly used in dissolution DNP.

The analysis in the previous paragraph neglects any changes in the coupling factor due to differing amounts of scalar and dipolar relaxation across the sample set. The scalar component is very hard to predict from molecular structure, as DMF has a structure similar to urea and acetone, but has dominantly scalar enhancement while urea and acetone do not. So while the connection between structure and an expected distance of closest approach in the previous paragraph seems reasonable, we realize that we cannot rule out a varying scalar contribution as the main determinant of ^{13}C DNP enhancement.

4. Conclusion

Urea dissolved in water gave the largest ^{13}C NMR signal enhancement through Overhauser-mediated DNP out of all the molecules studied. This can be attributed to a combination of two factors: a larger coupling factor than the other systems studied, which may be due to a smaller distance of closest approach or smaller scalar contribution, as well as a lower three-spin effect than for the other systems. The high enhancement of urea cannot be due to the presence of amide protons that undergo chemical exchange with the solvent. Even if the amide protons would display a strong NOE effect to ^{13}C , the enhancement would decrease due to a disadvantageous three-spin effect. Acetone and pyruvate gave moderate enhancement, while small enhancements were observed with methanol and DMF. The DNP enhanced signal of uniformly ^{13}C -labeled glucose was barely visible, due to a low leakage factor and the expected presence of a strong, unfavorable three-spin effect. All molecules exhibited DNP through a dipolar-mediated Overhauser effect except for DMF, which gave enhancement mediated by scalar relaxation.

Saturating the protons during a DNP experiment can help describe the relative magnitudes of the direct DNP term versus the three-spin term, and can increase the magnitude of the enhanced signal for systems with a dipolar coupling factor where the ^{13}C { ^1H } NOE exists but does not dominate the enhancement. Similarly, exchanging the H_2O solvent with D_2O will give a larger signal for dipolar coupled systems with existing three-spin effects, as long as the three-spin effect does not dominate the DNP enhancement.

Based on these experiments, the choice of a target molecule for optimal DNP polarization needs to be based on two considerations: (1) which molecule will have a small distance of closest approach, which may be determined from molecular dynamics simulations or might require systematic measurement, and (2) which molecule will minimize the often detrimental three-spin effect through hyperpolarized protons in close proximity to the ^{13}C site. The presence of scalar enhancement is very hard to predict, and a better understanding might require systematic studies of a wider range of molecules.

Due to the need to study many biological systems in their native environments, the use of dynamic nuclear polarization via the Overhauser effect to enhance the ^{13}C NMR signal under ambient conditions can be desirable. The observations and systematic approaches presented in this paper will be useful in finding, rational-

izing and optimizing a system that uses ^{13}C DNP in liquids via the Overhauser effect.

5. Experimental

5.1. Sample preparation

Urea- ^{13}C (99%) and sodium pyruvate-1- ^{13}C (99%) were obtained from Sigma-Aldrich/Isotec, while the *N,N*-dimethylformamide-carbonyl- ^{13}C (99%), acetone- $^{13}\text{C}_3$ (99%), methanol- ^{13}C and D_2O (99.9%) were purchased from Cambridge Isotope Laboratories (Andover, MA, USA). All were used as received, without further purification. All samples were dissolved at 5 M in deionized water or D_2O , with the exception of sodium pyruvate and the urea to which it was compared, which were 1 M concentrations. 4-Amino-2,2,6,6-tetramethylpiperidine-1-oxyl (4-amino-TEMPO, Sigma-Aldrich, USA) was also used as received, and was dissolved in solution at 20 mM for the comparison between molecules, and at variable concentrations for other experiments. The samples were not degassed.

The urea samples at different pH values were made by first creating a mixture of 20 mM 4-amino-TEMPO and 20 mM buffer (sodium citrate for pH 4 and 7, sodium carbonate for pH 10), then adjusting to the correct pH (± 0.1 pH unit). This mixture was then added to solid urea to form the final solution. Separate tests showed that adding urea to a solution does not appreciably change the pH.

5.2. DNP experiments

All DNP experiments were conducted in one of two systems. The first system consists of a commercial EMX ESR spectrometer and electromagnet (Bruker Biospin, Billerica, MA, USA). A homebuilt NMR probe was inserted into the commercial TE₁₀₂ resonant cavity. The resonance of the cavity and field of the center ESR transition were determined by the ESR spectrometer, then the field was set to the center transition and the cavity connected to a microwave source and custom, high-power microwave amplifier. The DNP experiment was performed in the resonant microwave cavity, with the addition of airflow through the cavity for sample cooling. The source and amplifier are capable of delivering up to 6 W of power to the sample, as described previously [12].

The second system uses a widebore 0.35 T superconducting magnet (Oxford Instruments, UK, formerly a 7 T magnet), with a homebuilt, variable frequency TE₁₀₂ resonant cavity. The variable cavity consisted of a length of WR90 waveguide, with flanges attached to both ends. On one end of the central waveguide, an iris plate (0.015" thick brass with a centered 6.85 mm hole) and a waveguide to coax adapter (RFAWA90, RF Lambda, Plano, TX, USA) were placed. On the other end, a cylindrical quarter wave backshort with a threaded support rod was held in the center of the waveguide via a threaded hole; this could be turned to vary the length and resonance frequency. All parts of the cavity were made of copper by a machine shop, as brass contains iron impurities which dramatically increase linewidths. The cavity was placed in the center of the magnet inside the room temperature shims from a Bruker 7T system (Avance 300 Spectrometer, 7T Ultrashield Widebore Magnet). A homebuilt NMR probe was inserted into the resonant cavity. The NMR resonance was found and used to calculate the electron resonance, the cavity was then tuned to the electron resonance frequency and on-resonant microwave radiation was applied with the custom microwave amplifier along with airflow through the cavity.

The electromagnet system was used when it was desired to measure an ESR spectrum concurrent with the DNP experiment,

and for experiments of a shorter duration. For longer experiments, it was found that the temperature dependence of the hall probe in the electromagnet caused field drift with subtle changes in the room temperature, which necessitated the construction of the system in the superconducting magnet. The superconducting magnet system was used for the comparisons between molecules, the decoupling experiments and the acquisition of unenhanced spectra. All other DNP data was collected with the electromagnet system.

For the double resonant experiments, such as the comparison between molecules or solvents, the NMR probe used was a double U-coil design, where the two U-loops were 1 cm long and 1 mm apart. The coil was connected via coaxial cable to a LC tuning circuit, then to a Kea NMR spectrometer (Magritek Limited, Wellington, New Zealand) operating at 3.73 MHz. An external amplifier was used for the ^{13}C pulse amplification (BT00250-Beta, Tomco Technologies, Norwood, SA, Australia). A simple 90° pulse and acquire sequence was employed.

For the triple resonant, proton-decoupling DNP experiments, a two-channel double U-coil NMR probe was constructed. The ^{13}C channel was connected in a manner similar to the double resonant experiments, and the ^1H channel was connected to another LC tuning circuit at 14.84 MHz, then to a homebuilt duplexer and another amplifier (BT00100-AlphaSA-CW, Tomco Technologies, Norwood, SA, Australia). A splitter on the spectrometer output allowed for the sending of signals to both channels. For decoupling, a MLEV-16 decoupling sequence [28] was applied for 5 times the length of the ^{13}C T_1 , and then the signal was read with a single pulse and acquisition on the carbon channel.

For DNP measurements, 4.0 μL of sample was placed in a 1 mm outer diameter quartz capillary (Vitrocomm, Mountain Lakes, NJ, USA). All DNP measurements are the average of at least two experiments, and the error is estimated at 15%. The sign of the enhancements with respect to equilibrium signal was obtained by measuring the unenhanced signal. This gave the sign, but the signal was too small to reliably integrate in some cases. The unenhanced signal of the methyl carbon of acetone was unobservable, so the sign was inferred from the decoupling experiments.

5.3. T_1 experiments

All T_1 experiments were conducted in the 0.35 T superconducting magnet, using a homebuilt ^{13}C NMR probe operating at 3.74 MHz. A Kea NMR spectrometer and external TOMCO amplifier were used for the experiments. Roughly 100 μL of sample was placed in a 5 mm NMR tube, and a simple inversion–recovery sequence was applied. The number of signal averages acquired for each delay value depended on the multiplicity of the ^{13}C resonance, concentration and volume of the sample, and varied from 16 to 148. The inversion–recovery curves were fit using Igor Pro (Wavemetrics, Inc., Portland, OR, USA). The error in the fit was less than 7% for all measurements.

5.4. Diffusion measurements

The diffusion coefficients for 5 M solutions of acetone, DMF and methanol were measured in the 0.35 T superconducting magnet with the X channel of a commercial 300 MHz solutions probe with gradients (Bruker Biospin) for ^1H detection at 14.85 MHz. A standard pulsed gradient sequence with stimulated spin echoes [29] was used, where the gradient strength was varied up to 3.7 G/mm, the duration between gradients was 50 ms, and the length of the gradient pulses was 5 ms. The data was processed in Prospa (Magritek Ltd).

The diffusion coefficient for urea was calculated from equations present in the literature [30], because a direct measurement is dif-

ficult due to the fast exchange of the amide protons. It was unfeasible to directly measure the diffusion coefficients of the 4-amino-TEMPO radical, because the signal from the radical at 20 mM concentrations is hidden underneath the signal from 5 M solute and the water signal, and the use of deuterated systems could produce incorrect results. Because of this, D_1 was calculated with the aid of the Stokes–Einstein equation, which relates diffusion coefficients and the fluid viscosity, η ,

$$D = \frac{k_B T}{6\pi\eta r}, \quad (7)$$

where r is the radius of the molecule. The diffusion coefficient of reduced 4-amino-TEMPO dissolved in water was directly measured to be $0.41 \times 10^{-9} \text{ m}^2/\text{s}$ by PGSE, then this number and the viscosity of water at 25°C were used with Eq. [7] to calculate the radius of the molecule, r . This value for the molecular radius was then placed back in Eq. [7] along with literature values of viscosity at 25°C for 5 M solutions of urea [31], acetone [32], DMF [33] or methanol [34] to calculate the diffusion coefficient for the radical in the systems of interest.

Acknowledgments

This work was supported by the University of California Cancer Research Committee (CRCC), the Faculty Early CAREER Award (20070057) of the National Science Foundation, and the Packard Fellowship for Science and Engineering. We thank Brandon Armstrong for helpful discussions of the theory, Craig Eccles and Andrew Coy of Magritek Ltd. for help with our pulse programs, and Bruce Dunson and Terry Hart of the UCSB Chemistry Machine shop for their help in designing and building the variable frequency cavity.

References

- [1] K.H. Hausser, D. Stehlik, Dynamic nuclear polarization in liquids, *Adv. Magn. Reson.* 3 (1968) 79–139.
- [2] W. Muller-Warmuth, K. Meise-Gresch, Molecular motions and interactions as studied by dynamic nuclear polarization (DNP) in free radical solutions, *Adv. Magn. Reson.* 11 (1983) 1–45.
- [3] R.A. Wind, M.J. Duijvestijn, C. van der Lugt, A. Manenschijn, J. Vriend, Applications of dynamic nuclear polarization in ^{13}C NMR in solids, *Prog. Nucl. Magn. Reson. Spectrosc.* 17 (1985) 33–67.
- [4] T. Maly, G.T. Debelouchina, V.S. Bajaj, K.-N. Hu, C.-G. Joo, M.L. MakJurkaskas, J.R. Sirigiri, P.C.A. van der Wel, J. Herzfeld, R.J. Temkin, R.G. Griffin, Dynamic nuclear polarization at high magnetic fields, *J. Chem. Phys.* 128 (2008) 052211.
- [5] G.J. Gerfen, L.R. Becerra, D.A. Hall, R.G. Griffin, R.J. Temkin, D.J. Singel, High frequency (140 GHz) dynamic nuclear polarization: polarization transfer to a solute in frozen aqueous solution, *J. Chem. Phys.* 102 (1995) 9494–9497.
- [6] K.H. Tsai, H.C. Dorn, A model for establishing the ultimate enhancements in the low to high magnetic field transfer dynamic nuclear polarization experiment, *Appl. Magn. Reson.* 1 (1990) 231–254.
- [7] J.H. Ardenkjaer-Larsen, B. Fridlund, A. Gram, G. Hansson, L. Hansson, M.H. Lerche, R. Servin, M. Thaning, K. Golman, Increase in signal-to-noise ratio of $>10,000$ times in liquid-state NMR, *Proc. Nat. Acad. Sci. USA* 100 (2003) 10158–10163.
- [8] K. Golman, J.H. Ardenaer-Larsen, J.S. Petersson, S. Mansson, I. Leunbach, Molecular imaging with endogenous substances, *Proc. Nat. Acad. Sci. USA* 100 (2003) 10435–10439.
- [9] K. Golman, R. In't Zandt, M. Thanning, Real-time metabolic imaging, *Proc. Nat. Acad. Sci. USA* 103 (2006) 11270–11275.
- [10] E.R. McCarney, S. Han, Spin-labeled gel for the production of radical-free dynamic nuclear polarization enhanced molecules for NMR spectroscopy and imaging, *J. Magn. Reson.* 190 (2008) 307–315.
- [11] E.R. McCarney, B.D. Armstrong, M.D. Lingwood, S. Han, Hyperpolarized water as an authentic magnetic resonance imaging contrast agent, *Proc. Nat. Acad. Sci. USA* 104 (2007) 1754–1759.
- [12] B.D. Armstrong, M.D. Lingwood, E.R. McCarney, E.R. Brown, P. Blümler, S. Han, Portable X-band system for solution state dynamic nuclear polarization, *J. Magn. Reson.* 191 (2008) 273–281.
- [13] N.M. Loening, M. Rosay, V. Weis, R.G. Griffin, Solution-state dynamic nuclear polarization at high magnetic field, *J. Am. Chem. Soc.* 124 (2002) 8808–8809.
- [14] S. Stevenson, H.C. Dorn, ^{13}C dynamic nuclear polarization: a detector for continuous-flow, online chromatography, *Anal. Chem.* 66 (1994) 2993–2999.

- [15] T.C. Cannon, R.E. Richards, D. Taylor, Enhancement and reversal of carbon-13 resonances in nuclear-electron double resonance, *J. Chem. Soc. A* (1970) 1180–1184.
- [16] W. Muller-Warmuth, R. Vilhjalmsson, P.A.M. Gerlof, J. Smidt, J. Trommel, Intermolecular interactions of benzene and carbon tetrachloride with selected free radicals in solution as studied by ^{13}C and ^1H dynamic nuclear polarization, *Mol. Phys.* 31 (1976) 1055–1067.
- [17] D. Neuhaus, M.P. Williamson, *The Nuclear Overhauser Effect in Structural and Conformational Analysis*, Wiley-VCH, New York, 2000.
- [18] E.R. McCarney, B.D. Armstrong, R. Kausik, S. Han, Dynamic nuclear polarization enhanced nuclear magnetic resonance and electron spin resonance studies of hydration and local water dynamics in micelle and vesicle assemblies, *Langmuir* 24 (2008) 10062–10072.
- [19] B. Borah, R.G. Bryant, NMR relaxation dispersion in an aqueous nitroxide system, *J. Chem. Phys.* 75 (1981) 3297–3300.
- [20] B.D. Armstrong, S. Han, A new model for Overhauser enhanced nuclear magnetic resonance using nitroxide radicals, *J. Chem. Phys.* 127 (2007) 104508.
- [21] R.D. Bates, W.S. Drozdowski, Use of nitroxide spin labels in studies of solvent-solute interactions, *J. Chem. Phys.* 67 (1977) 4038–4044.
- [22] H.C. Dorn, J. Gu, D.S. Bethune, R.D. Johnson, C.S. Yannoni, The nature of fullerene solution collisional dynamics. A ^{13}C DNP and NMR study of the C60/C6D6/TEMPO system, *Chem. Phys. Lett.* 203 (1993) 549–554.
- [23] K.H. Hausser, F. Reinbold, Dynamic polarisation in a three-spin system, *Phys. Lett.* 2 (1962) 53–54.
- [24] H. Brunner, K.H. Hausser, Dynamic nuclear polarization of protons, ^{19}F and ^{13}C nuclei at 21 kG, *J. Magn. Reson.* 6 (1972) 605–611.
- [25] B.D. Armstrong, P. Soto, J. Shea, S. Han, Overhauser dynamic nuclear polarization and molecular dynamics simulations using pyrroline and piperidine ring nitroxide radicals, *J. Magn. Reson.* 200 (2009) 137–141.
- [26] J.A. Weil, J.R. Bolton, J.E. Wertz, *Electron Paramagnetic Resonance. Elementary Theory and Practical Applications*, Wiley, New York, 1994.
- [27] R.L. Vold, E.S. Daniel, S.O. Chan, Magnetic resonance measurements of proton exchange in aqueous urea, *J. Am. Chem. Soc.* 92 (1970) 6771–6776.
- [28] M.H. Levitt, R. Freeman, T. Frenkiel, Broadband heteronuclear decoupling, *J. Magn. Reson.* 47 (1982) 328–330.
- [29] J.E. Tanner, Use of the stimulated echo in NMR diffusion studies, *J. Chem. Phys.* 52 (1970) 2523–2526.
- [30] J.G. Albright, R. Mills, A study of diffusion in the ternary system, labeled urea-urea-water, at 25 by measurements of the intradiffusion coefficients of urea, *J. Phys. Chem.* 69 (1965) 3120–3126.
- [31] K. Kawahara, C. Tanford, Viscosity and density of aqueous solutions of urea and guanidine hydrochloride, *J. Biol. Chem.* 241 (1966) 3228–3232.
- [32] K.S. Howard, R.A. McAllister, The viscosity of acetone-water solutions up to their normal boiling points, *AIChE J.* 4 (1958) 362–366.
- [33] J.M. Bernal-García, A. Guzmán-López, A. Cabrales-Torres, A. Estrada-Baltazar, G.A. Iglesias-Silva, Densities and viscosities of (*N,N*-dimethylformamide + water) at atmospheric pressure from (283.15 to 353.15) K, *J. Chem. Eng. Data* 53 (2008) 1024–1027.
- [34] H. Colin, J.C. Diez-Masa, G. Guiochon, T. Czejkwiska, I. Miedziak, The role of the temperature in reversed-phase high-performance liquid chromatography using pyrocarbon-containing adsorbents, *J. Chromatogr.* 167 (1978) 41–65.